

Article

Properties and Mechanical Strength Analysis of Concrete Using Fly Ash, Ground Granulated Blast Furnace Slag and Various Superplasticizers

Chuen-UI Juang and Wen-Ten Kuo * 

Department of Civil Engineering, National Kaohsiung University of Science and Technology, Kaohsiung 807, Taiwan; vivian820830@gmail.com

* Correspondence: wtkuo@nkust.edu.tw

Abstract: Supplementary cementitious materials (SCMs) have been widely used to replace cement in recent years in order to reduce the burden of cement on the environment. In this study, fly ash (FA) and ground-granulated blast furnace slag (GGBFS) were used as long-term 40%, 50% and 60% replacement cement in order to explore the mechanical strength of different superplasticizers (SPs) under high substitution amounts. The results of the study showed that, in terms of the nature of work, when 60% of cement was replaced with SCM, the initial setting time was increased by 40–70 min. The values of the ratio of the initial to final setting time (I/F ratio) are equivalent when the I/F values of PCE and SNF are at $W/B = 0.27$ and 0.35 , and at the lowest W/B (0.21) in this study, the I/F calculation result was the difference between PCE and MLS. The I/F value is equal, which means that when the W/B is low, PCE and MLS have the same impact on workability, and as W/B increases, the impact of PCE and SNF is similar. In terms of compressive strength, $W/B = 0.21$. The 1-day curing age of PCE was compared with the 91-day curing age, and it was found that at high volumes of replacement, increasing GGBFS by 10% can increase the strength by 37%. Using the ultrasonic wave velocity as the input value and the compressive strength result as the output value, the MATLAB back propagation neural network prediction model was carried out. The best correlation coefficient R value of MLS was 0.97, and the mean squared error was 2.21, which has good prediction ability.

Keywords: fly ash; ground-granulated blast furnace slag; superplasticizer; ternary compound concrete; back propagation neural network



Citation: Juang, C.-U.; Kuo, W.-T. Properties and Mechanical Strength Analysis of Concrete Using Fly Ash, Ground Granulated Blast Furnace Slag and Various Superplasticizers. *Buildings* **2023**, *13*, 1644. <https://doi.org/10.3390/buildings13071644>

Academic Editor: Jan Fort

Received: 6 June 2023

Revised: 23 June 2023

Accepted: 26 June 2023

Published: 28 June 2023



Copyright: © 2023 by the authors. Licensee MDPI, Basel, Switzerland. This article is an open access article distributed under the terms and conditions of the Creative Commons Attribution (CC BY) license (<https://creativecommons.org/licenses/by/4.0/>).

1. Introduction

A low-carbon circular economy is a goal that the whole world is striving to achieve. Similarly, the construction industry wants to meet this goal in terms of its widely used cement-related products and to thus reduce the negative effects of cement manufacturing on the environment and create a sustainable, environmentally friendly, and green-energy-based environment. During the cement manufacturing process, approximately 0.9 metric tons of CO_2 are emitted into the atmosphere for every metric ton of cement produced [1]. Cement, an adhesive in concrete, is one of the primary reasons for the considerable amounts of greenhouse gases generated by the construction industry [2]. Therefore, the most effective method for decreasing the harmful effects of greenhouse gases on the atmosphere by reducing greenhouse gas emissions is to replace cement with materials that have cement-like properties [3]. Supplementary cementitious material (SCM), as a substitute for concrete, can effectively reduce environmental impact and protect natural resources. Most of the basic components of SCM are pozzolanic, which can effectively increase the late strength of concrete, improve the microstructure, and reduce greenhouse gas emissions [4].

Fly ash (FA) is a type of ash produced by coal-fired power plants and is commonly used as a SCM inside cement-based materials. In industry, it is commonly believed that when replacing cement with FA, 10–30% should be used [5,6]. Scholars have studied

high-volume fly ash (HVFA) concrete [7,8], an environmentally friendly material, and investigated its suitability as a sustainable material for the construction industry. HVFA concrete can be developed that has the ideal mechanical properties and durability [9–12]. Bouzoubaâ et al. [13] replaced 50% of the mass of cement used with FA under the condition of a water/cement ratio (W/C) of 0.42 and found that after the material had been cured for 56 and 91 days, it exhibited a compressive strength of 32.2 and 35.2 MPa, respectively, values that are considerably superior to those of ordinary Portland cement (OPC) concrete without FA under the condition $W/C = 0.53$. Mardani-Aghabaglou and Ramyar [14] indicated that when 60% of cement is replaced with FA, the material that results after 180 days of curing has 15–18% higher compressive strength than does OPC. Chen et al. [15] reported that replacing 50–80% of cement with FA reduced the rate of drying shrinkage by roughly 23–30%. Müllauer et al. [16] discovered that replacing 70% of cement with FA effectively inhibited alkali–aggregate reactions. Wang et al. [17] used finely ground phosphorus slag (FGPS) and FA to investigate the durability of hydraulic concrete; their results show that adding FGPS and FA can help reduce the pore structure of concrete, and the optimal replacement amounts are 30% of FGPS and 15% of FA. Wang et al. [18] discussed the influence of FA on the permeability of panel concrete. Their research results showed that the optimal FA addition amount is 30%, and under long-term maintenance, it can effectively improve the development of compressive strength.

Ground-granulated blast furnace slag (GGBFS) is one of the waste products of blast furnace ironmaking. When making iron, glassy blast furnace slag is produced following water quenching and cooling. GGBFS has been widely used as a replacement for cement to glue materials together and has been found to exhibit remarkable gluing effects. Crossin [19] reported that using GGBFS as an SCM could lead to a decrease in greenhouse gas emissions of 47.5%. Using a higher GGBFS content when fabricating ternary mixed cement led to cement with higher mechanical strength compared to that of OPC when the curing period was 28 days [20–22]. Lim et al. [23] noted that ternary mixed cement made using GGBFS initially had a compressive strength lower than that of OPC because of the OPC dilution effect. However, after a curing period of 28–365 days, the compressive strength was greater than that of OPC [20]; the increase in compressive strength is most substantial for a curing period of 28–91 days [21–24]. Cheah et al. [25] produced ternary mixed cement mortar by using cement, ground coal bottom ash (GCBA), and GGBFS. Their results showed that the optimal mix ratio was 40% GGBFS and 5% GCBA if no superplasticizer (SP) was added and 40% GGBFS and 10% GCBA if SP was added. These findings revealed that the two SCMs can effectively enhance the physical and mechanical properties of cement mortar [26]. Through the research on ternary cementitious materials (GGBFS and silica fume) and waste concrete aggregates, it was found that effectively replacing cement with 25% GGBFS can effectively increase the global warming potential value. Weise et al. [27] explored the effect of the addition of metakaolin on OH addition. The study showed that the addition of metakaolin was 30 wt%, and the consumption of CH was the largest at the age of 28 days and 56 days and the slowest at the age of 28 days. CH will be completely consumed after the period, causing the strength to be affected. SCMs have a high amount of metakaolin, which can improve the cement reaction in concrete [28].

Although many scholars have conducted correlation studies on various SCMs, few have investigated the effects of high GGBFS and FA replacement ratios on the engineering properties of various SP agents. As the use of environmentally friendly materials as building materials becomes increasingly popular, replacing cement with SCMs in high ratios will inevitably become a future development trend. Accordingly, this study replaced over 50% of cement with GGBFS and FA (in accordance with the weights of cementing materials) and with HVFA and GGBFS concrete (HVFGC) fabricated using three SP agents at low water-to-binder (W/B) ratios; the engineering properties (e.g., workability, mechanical properties, and durability) of the mixed materials were then examined.

2. Methods

2.1. High Volume Fly Ash and Ground Granulated Blast-Furnace Slag Concrete Material Preparation

The HVFGC cementitious materials produced in this study were mixtures of OPC, GGBFS, and FA, whereas the pellets that were fabricated were made of natural sand from Ligang Township, Taiwan. The SP employed, provided by Yo Rich (Taipei, Taiwan), had a solid content of 34.4%; the polycarboxylate superplasticizer (PCE), a light yellow liquid, had a water reduction rate of 26.9%; the sulphonated naphthalene formaldehyde (SNF) condensate, a dark brown liquid, had a water reduction rate of 23.6%; and the modified salt of lignosulfonates (MLS), a brown liquid with a pungent smell, had a water reduction rate of 12.2%. Detailed information on the materials is provided in the following subsections.

2.1.1. Cementitious Materials

In this study, the cement used was Type 1 Portland cement provided by the Southeast Cement Corporation (Kaohsiung, Taiwan); this cement conformed to the ASTM C150 guidelines [29]. The FA used was Class F coal fly ash, a recycled and environmentally friendly material provided by the Taiwan Power Company; this FA conformed to the ASTM C618 guidelines [30]. The GGBFS, provided by the China Steel Corporation (Kaohsiung, Taiwan) conformed to the ASTM C989 guidelines [31]. The composition of the HVFGC cementitious materials is detailed in Table 1.

Table 1. HVFGC materials chemical and physical composition.

Chemical Composition (%)		Cement	FA	GGBFS
	SiO ₂	21.23	67.9	34.4
	Al ₂ O ₃	5.57	21.5	14.8
	Fe ₂ O ₃	3.57	3.63	0.41
	CaO	62.15	2.1	41.7
	MgO	2.51	1.2	6.6
	SO ₃	1.99	0.26	0.12
	Na ₂ O	0.1	0.68	0.28
	K ₂ O	0.54	0.84	0.37
Physical property	Fineness (m ² /kg)	321	381.8	400
	Specific gravity	3.15	2.16	2.90
	Alkali content (%)	-	1.23	0.52
	LOI	2.65	2.8	-

2.1.2. Natural Aggregate

The coarse and fine aggregates used in the experiment were all natural river sand collected from Ligang Township, Pingtung County, Taiwan. The aggregate particle sizes conformed to the ASTM C33 [32] gradation curve guidelines. The coarse aggregate, which was obtained by collecting the aggregate that did not pass through a 3/8" sieve #4, had a specific gravity and water absorption rate of 2.65 and 1.71%, respectively (Figure 1). By contrast, the fine aggregate had a specific gravity and water absorption rate of 2.61 and 1.92%, respectively (Figure 2).



Figure 1. Coarse aggregate.



Figure 2. Fine aggregate.

2.2. Mixing Proportions and Specimen Preparation

This study investigated the effects of adding high ratios of pozzolanic materials and SPs to high-performance concrete. The ratios were calculated using the volume method and low W/B ratios of 0.21, 0.27, and 0.35. Fixed amounts (i.e., 2%) of PCE, SNF, and MLS were added, where the ratios of FA and GGBFS that replaced the cement were set at either 20% or 30%. The different ratios of cement replaced in the experiment are shown in Table 2.

Table 2. Experimental variables and codes.

Variable	Value
W/B	0.21, 0.27, 0.35
FA (%)	20, 30
GGBFS (%)	20, 30
Code	For example: 21F20S30, then W/B = 0.21, FA substitution amount is 20%, GGBFS substitution amount is 30%.

A cubic test object measuring 50 mm × 50 mm × 50 mm, and 40 mm × 40 mm × 160 mm flexural test was used to test the mechanical properties and durability of the materials used in the experiments. Relevant compression tests were performed for curing periods of 1, 7, 28, 56, and 91 days. HVFGC samples were mixed using a 12 L mortar mixer and by adopting the following procedure: (1) the coarse and fine aggregates were dry-mixed evenly, 1/3 of mixing water was added, and the mixture was then stirred at a speed of 100 rpm for approximately 2 min to make the aggregates moist; (2) the premixed cementitious materials were added, and the mixture was stirred at a speed of 100 rpm for 5 min; and (3) the SP agents were added, and mixing was continued at 100 rpm for 5 min. The samples were removed from the mold once they had entered a solid state (after 24 h), and the samples were cured in saturated limewater until the time of the experiments.

2.3. Methods

The HVFGC was mixed following the procedure specified in ASTM C305 [33]. To identify the HVFGC's construction workability, the fresh mix setting time (ASTM C807) [34] was determined. Regarding engineering properties, the compressive strength (ASTM C109) [35], flexural strength (ASTM C348) [36], ultrasonic wave velocity (ASTM C597) [37], and water absorption rate (ASTM C1585) [38] were determined. Neural network simulations were performed to establish related prediction models, and microscopic analyses were conducted using scanning electron microscopy (SEM) and X-ray diffraction.

The back propagation neural network (BPNN) was analyzed by Matlab to explore the prediction model of ultrasonic wave velocity and compressive strength in this experiment. The basic assumptions for model establishment were: (1) the number of neurons in the hidden layer was 2; (2) the number of training times was 10,000; (3) the minimum error converged to 0.0001; (4) the learning rate was 0.1; (5) the inertia factor was 0.5; (6) the

relationship between the input layer and the hidden layer was logsig; (6) the relationship between the hidden layer and the output layer was purelin.

3. Results and Discussion

3.1. HVFGC Workability

Figures 3–5 show the time it took for PCE, SNF, and MLS to set in the experiments, respectively. As the W/B ratio was decreased, the setting time decreased, especially the initial setting time, for which the effect was strongest for SNF. When the W/B ratio was decreased from 0.35 to 0.21, the initial setting time for SNF, MLS, and PCE decreased by 2.56, 1.54, and 1.25 times, respectively. When the W/B ratio was 0.35, the final setting time of MLS exceeded 1400 min. This is unsuitable in engineering practice because an overly long final setting time affects the mechanical properties of HVFGC. The ratio of the initial to final setting time (I/F ratio) was calculated and revealed that when 50% of cement was replaced with SCM, the I/F values were similar regardless of whether the cement was replaced with FA at a higher ratio than it was with GGBFS (or whether the cement was replaced with GGBFS at a higher ratio than it was with FA), that is, F20F30 and F30S20 had similar I/F values. When the I/F values of PCE and SNF are at W/B = 0.27 and 0.35, the I/F values of the two materials are equivalent, and the lowest W/B = 0.21 in this study. The I/F calculation result is the difference between PCE and MLS. The I/F value is equal, which means that when the W/B is low, PCE and MLS have the same impact on workability, and as W/B increases, the impacts of PCE and SNF are similar. Although PCE and SNF had similar final setting times, the initial setting time of PCE was approximately 2 h shorter than that of SNF, which indicated unfavorable workability. When the amount of SCM that replaced cement was increased to 60%, the initial setting time increased by roughly 40–70 min, signifying that the decrease in cement specific surface area slowed the hydration heat release [39,40].

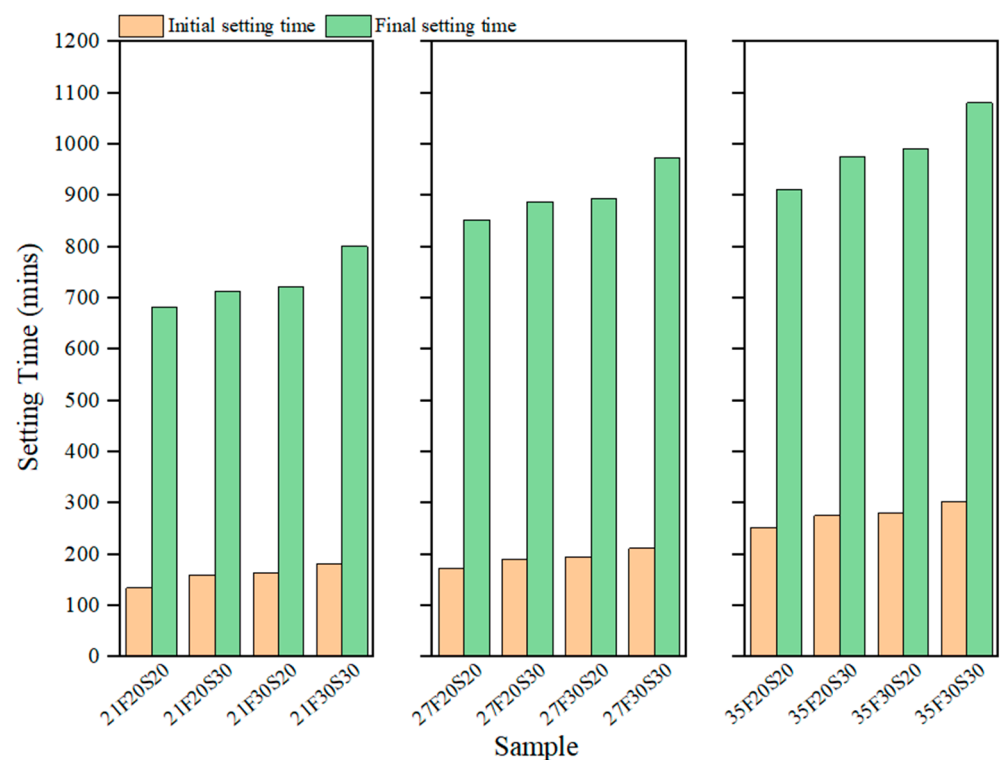


Figure 3. Setting time of HVFGC adding PCE with different W/B.

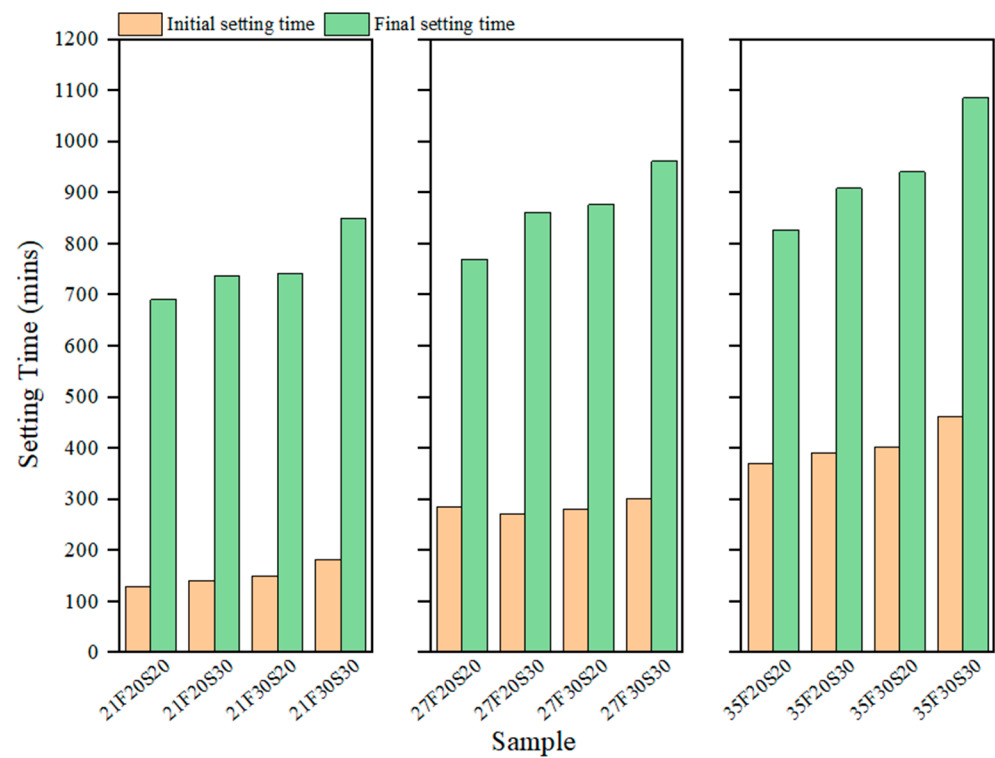


Figure 4. Setting time of HVFGC adding MLS with different W/B.

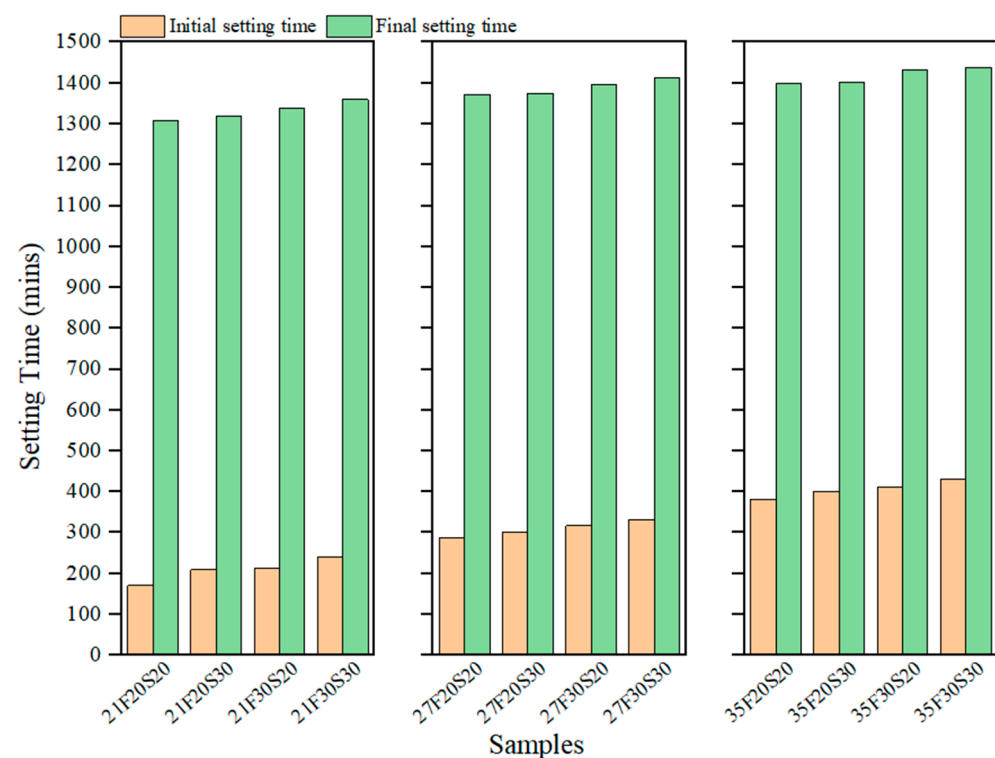


Figure 5. Setting time of HVFGC adding SNF with different W/B.

3.2. HVFGC Mechanical Behavior to Compressive Strength

The mechanical behavior of HVFGC was determined using compressive strength and flexural strength tests. The compressive strength of PCE, SNF, and MLS are shown in Figures 6–8, respectively. As the percentage of SCM was increased, the compressive strength decreased. The optimal compressive strength (79.93 MPa) was achieved using

PCE, a curing period of 91 days, a W/B ratio of 0.21, and FA and GGBFS replacement ratios of 20% and 20%, respectively. The strength development of PCE and SNF was more pronounced from Days 1 to 7, whereas that of MLS was most pronounced from Days 7 to 28. The strength development of MLS slowed considerably after Day 28 and increased again after Day 56. These phenomena were primarily caused by the SCM triggering pozzolanic reactions, which produced secondary hydrations that contributed to strength development. When the SCM replaced 60% of the cement, the strength development was the most pronounced from Days 28 to 56. In engineering practice, PCE and SNF are suitable for engineering projects needing rapid early-stage strength development. Conversely, MLS is suitable for engineering projects that require late-stage strength development. Concerning the effects of the ratios of FA and GGBFS used in addition to SP, for PCE, when 20% of the cement was replaced with FA, an increase in the ratio of cement-replacing GGBFS resulted in an improvement in strength development. This finding supported that of Manojsuburam et al. [41], who reported that under the interaction between the two-phase SCM materials FA and GGBFS, GGBFS can effectively accelerate strength development [42,43]. In this study, taking $W/B = 0.21$ as an example, the 1-day curing age of PCE was compared with the 91-day curing age, and it was found that at high volume replacement, increasing GGBFS by 10% can increase the strength by 37%.

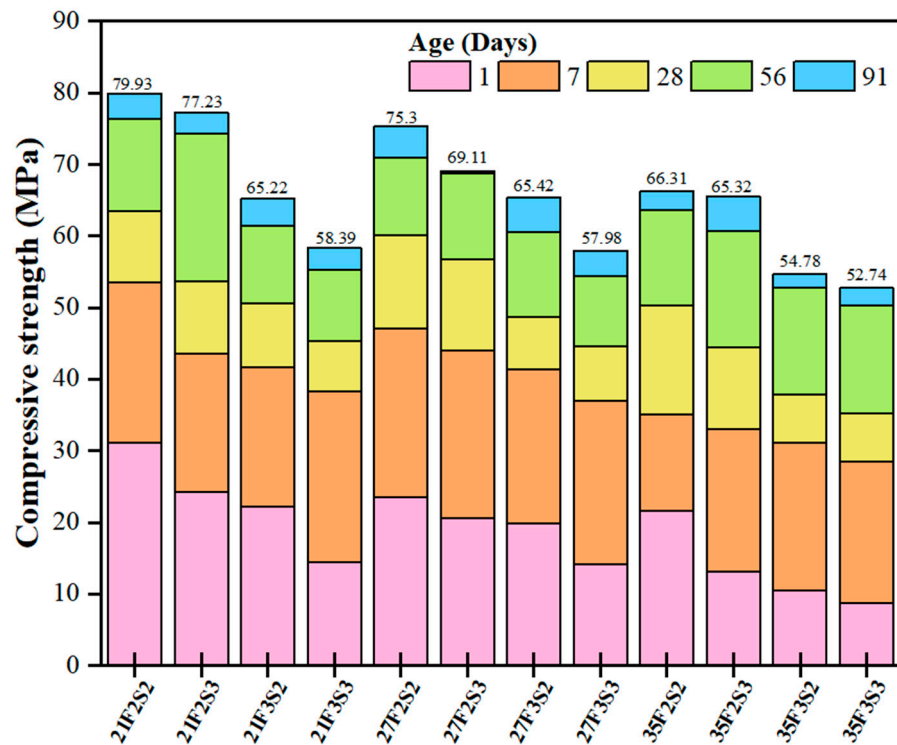


Figure 6. Growth of compressive strength in different curing ages by adding PCE to HVFGC.

3.3. HVFGC Mechanical Behavior to Flexural Strength

The flexural strengths of PCE, SNF, and MLS are illustrated in Figures 9–11, respectively. The optimal flexural strength was 18.75, 19.31, and 18.75 MPa for PCE, MLS, and SNF, respectively. Such flexural strength was achieved using a W/B ratio of 0.21 and FA and GGBFS replacement ratios of 20% and 20%, respectively. As the percentage of cement that was replaced with SCM was increased, the flexural strength decreased. The strength development increased the most rapidly from Days 1 to 7 and slowed as the curing period progressed. For MLS, when 30% and 30% of cement was replaced with FA and GGBFS, respectively, the strength development from Days 1 to 7 was approximately 33.9% higher than when 20% and 20% of cement were replaced with FA and GGBFS, respectively. This phenomenon was mainly because of the effects of FA, which increased strength develop-

ment [44]. Nevertheless, at a curing period of 56 days, a change in the ratio of SCM that replaced cement did not result in a significant change in flexural strength [45–48].

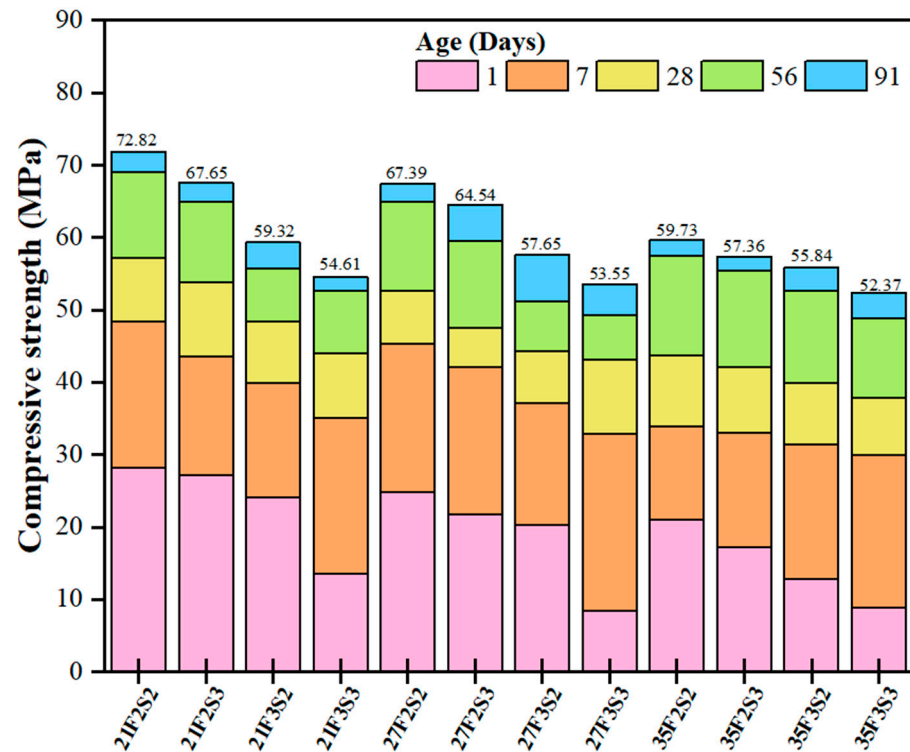


Figure 7. Growth of compressive strength in different curing ages by adding MLS to HVFGC.

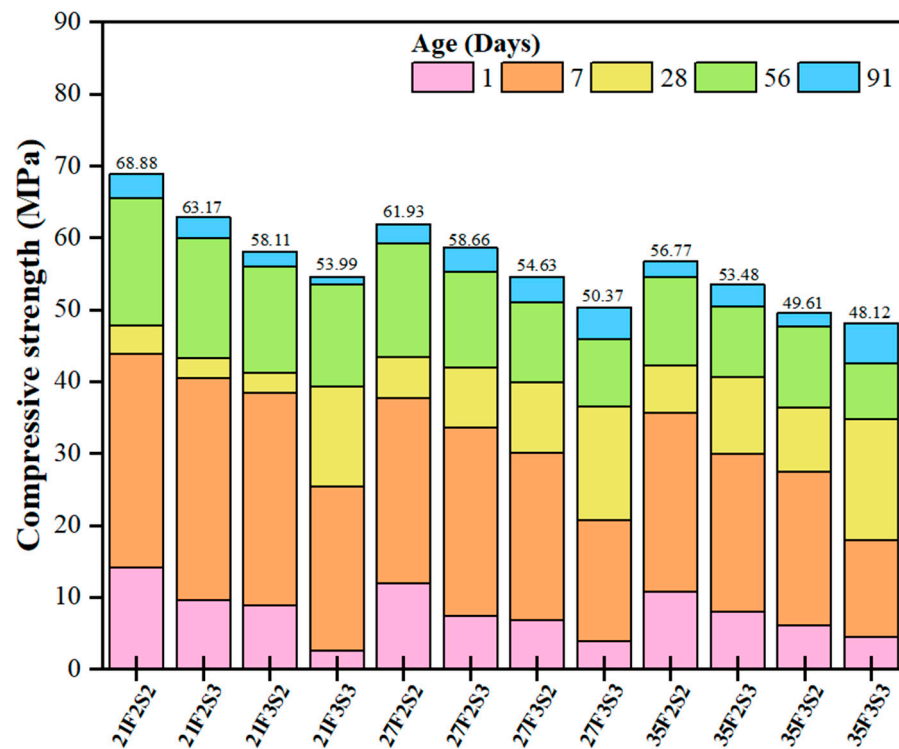


Figure 8. Growth of compressive strength in different curing ages by adding SNF to HVFGC.

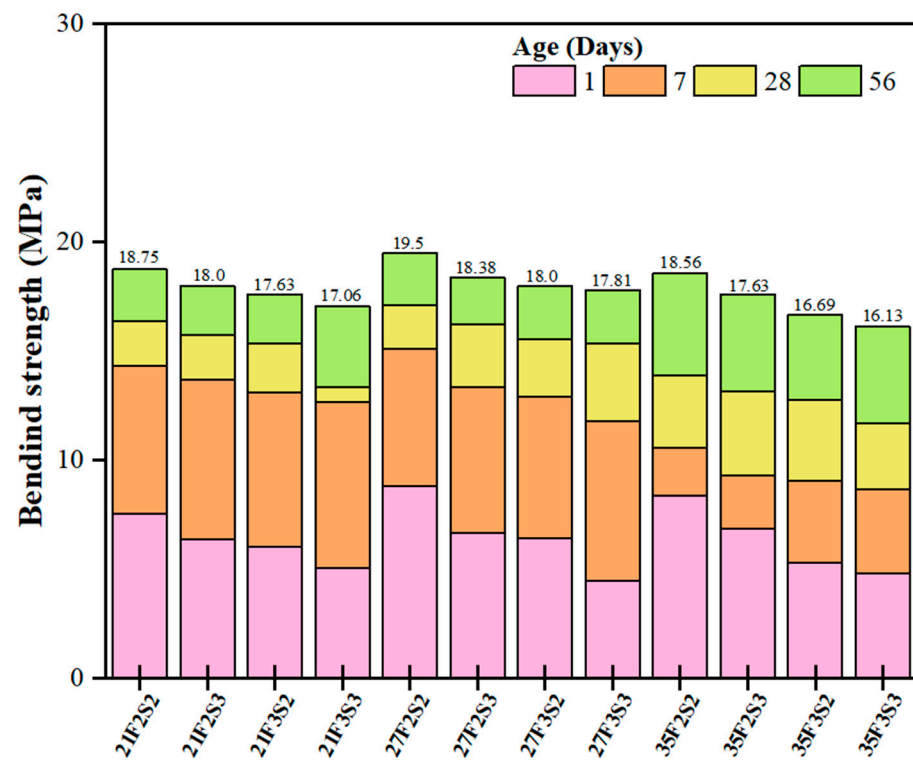


Figure 9. HVFGC added PCE bending strength growth in different curing ages.

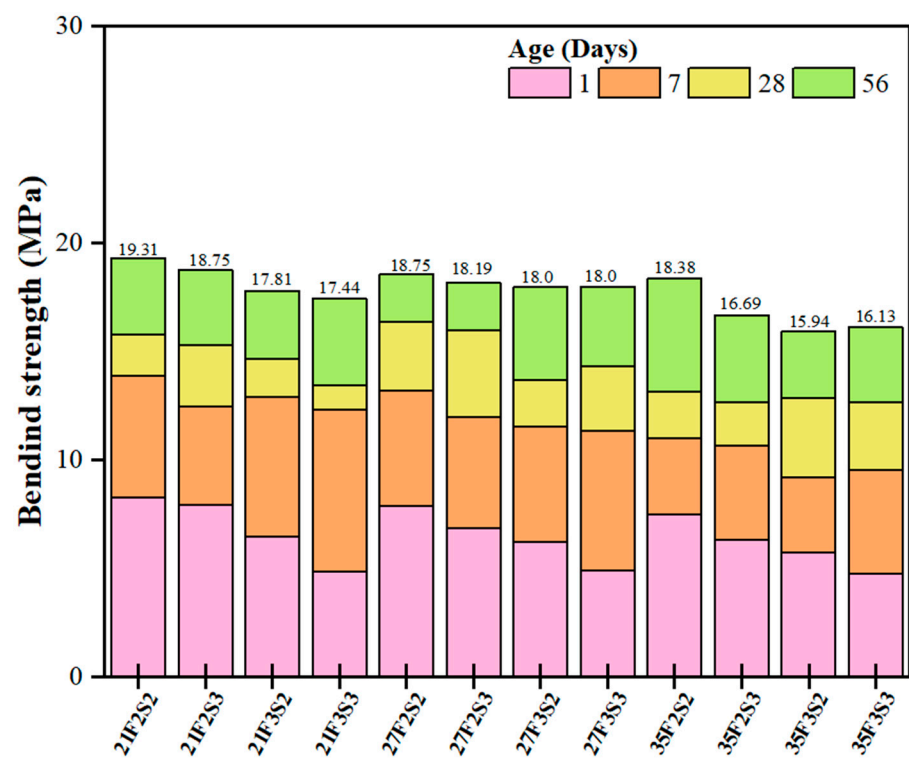


Figure 10. HVFGC added MLS bending strength growth in different curing ages.

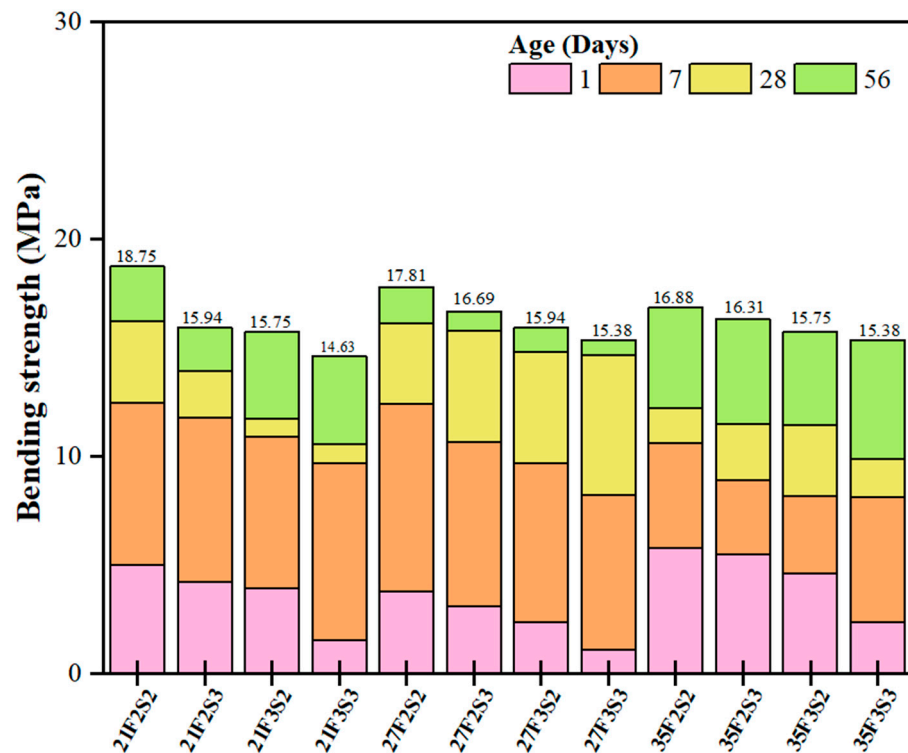


Figure 11. HVFGC added SNF bending strength growth in different curing ages.

3.4. Nondestructive Experiments and Mechanical Behavior

Ultrasonic wave velocities were used in nondestructive experiments, which were performed to determine how nondestructive experiments affect HVFGC compressive strength; the findings can provide reference information for future projects. Figures 12–14 show the ultrasonic wave velocity experimental results. As the percentage of cement that was replaced with SCM was increased, the ultrasonic wave velocity decreased; as the W/B ratio was increased, the ultrasonic wave velocity and compressive strength increased. We used the ultrasonic wave velocity and compressive strength values to develop a MATLAB backward transfer neural network prediction model. The results of the prediction model are illustrated in Figures 15–17. The predicted R value represents the correlation of the test values of the predicted results. In the results of the prediction model of this study, the R value of PCE is 0.96; the R value of MLS is 0.97; and the R value of SNF is 0.96. The three test results are all highly reliable and can be used as a reference for future engineering applications. The MLS R value of 0.97 is the highest value of the three SPs, and the corresponding mean squared error is 2.21.

3.5. Comprehensive Assessment of the Microscopic Analyses

We used microscopic analyses as a comprehensive platform to assess engineering properties. Microscopic analyses were conducted on the test objects when using a curing period of 28–56 days. The results are shown in Figure 18. The MLS sample had more pores than the other samples, which explained why its compressive strength was lower. Comparing the SEM images for curing periods of 28 and 56 days revealed that, for a curing period of 28 days, the FA sample had not been fully hydrated, which diminished the effects of FA on strength development.

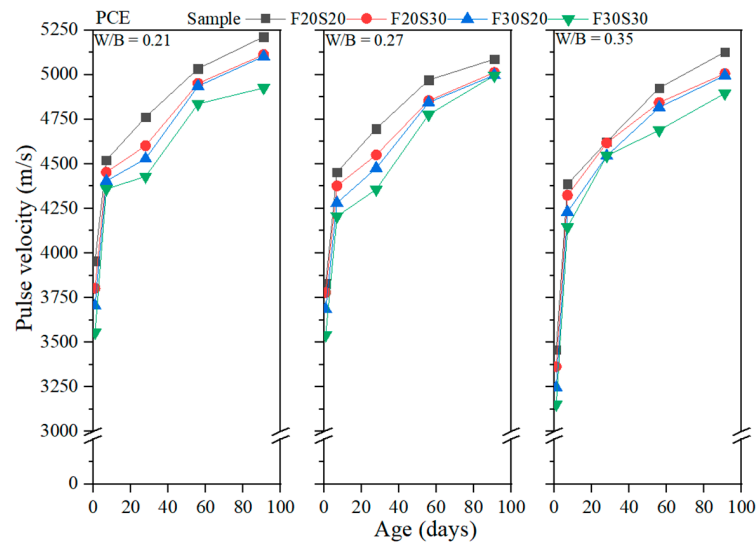


Figure 12. Ultrasonic wave velocities of HVFGC adding PCE with different substitution amounts.

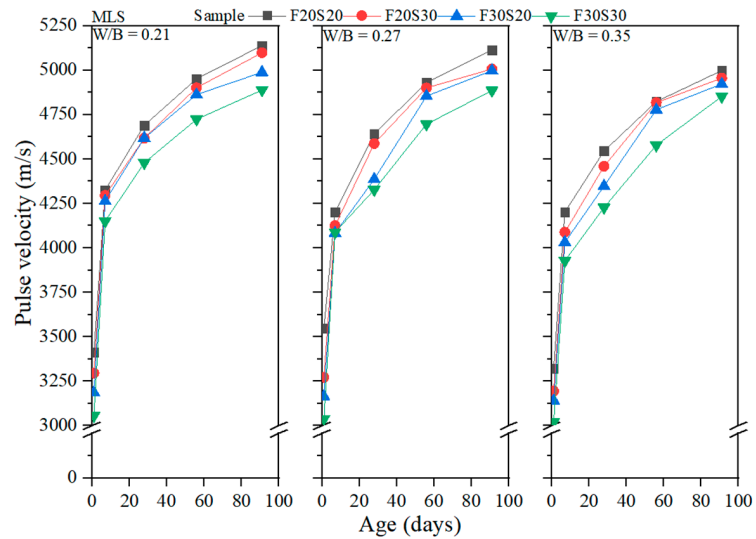


Figure 13. Ultrasonic wave velocities of HVFGC adding MLS with different substitution amounts.

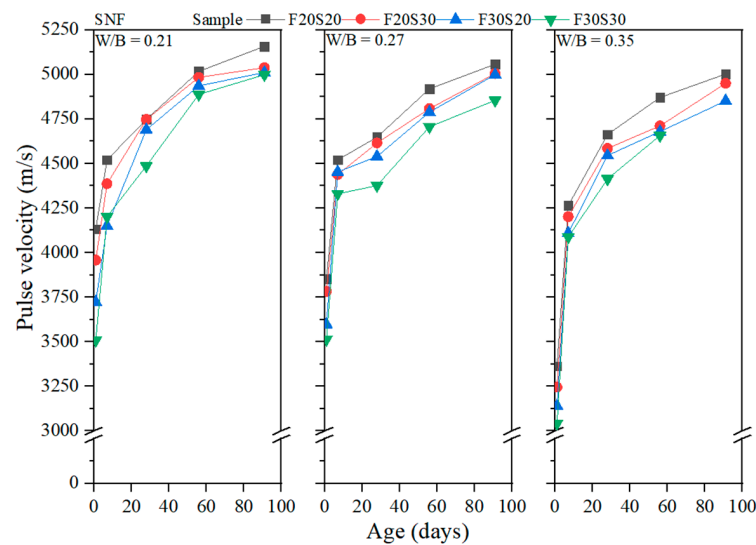


Figure 14. Ultrasonic wave velocities of HVFGC adding SNF with different substitution amounts.

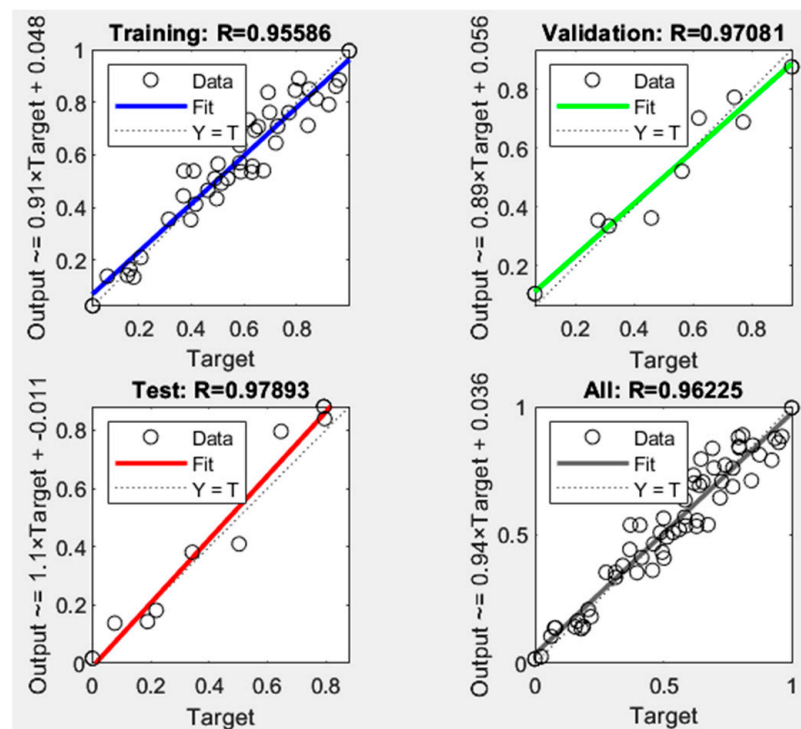


Figure 15. HVFGC back propagation neural network prediction model of PCE.

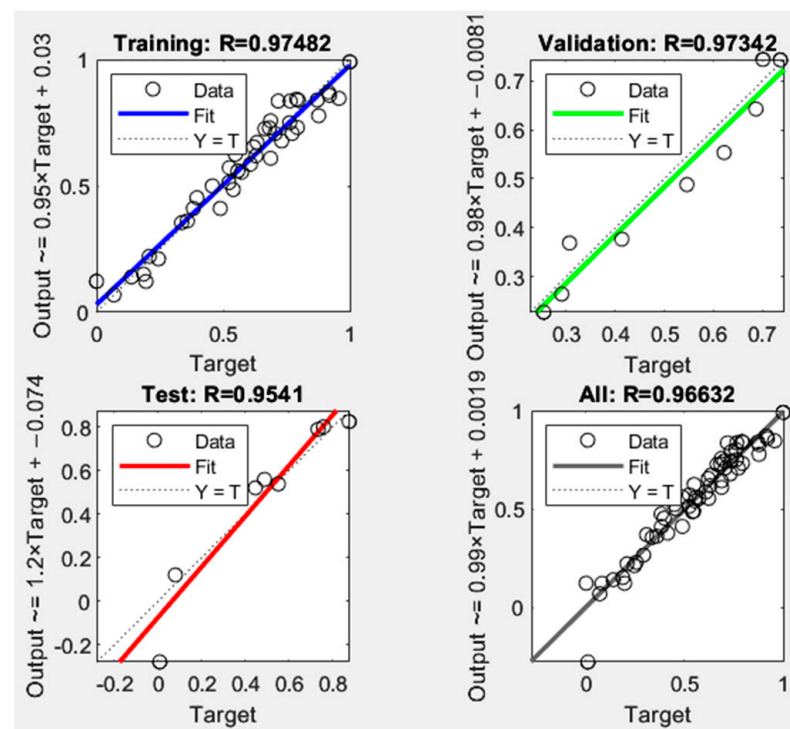


Figure 16. HVFGC back propagation neural network prediction model of MLS.

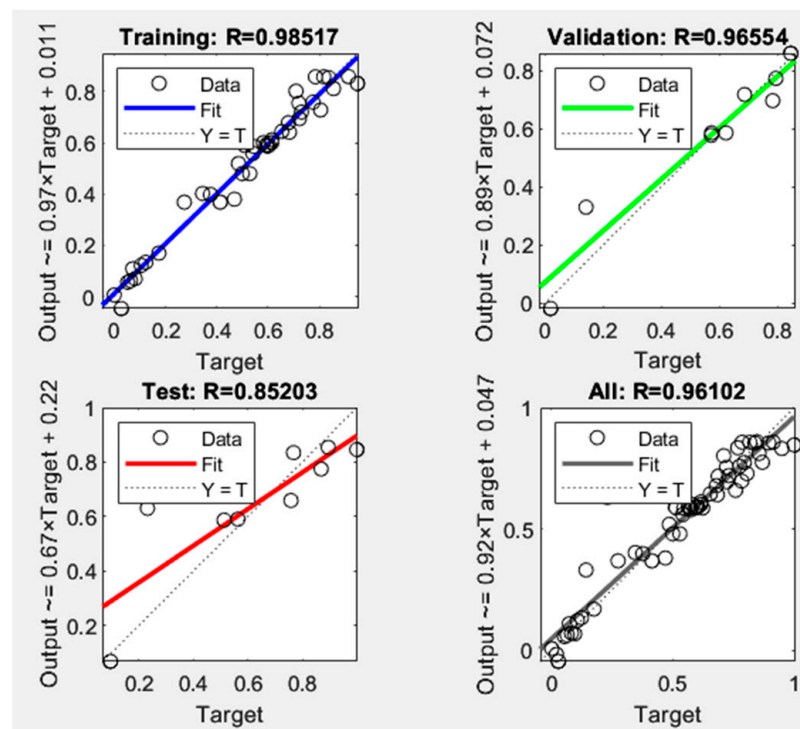


Figure 17. HVFGC back propagation neural network prediction model of SNF.

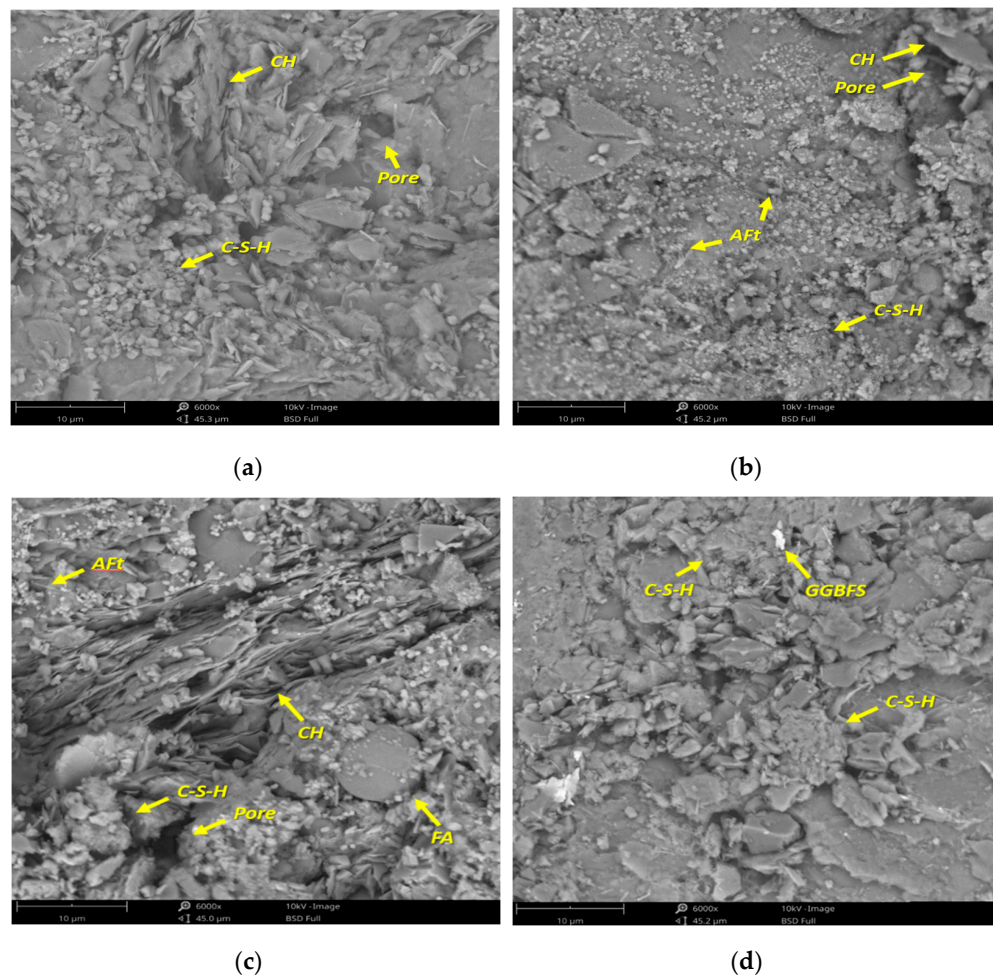


Figure 18. Cont.

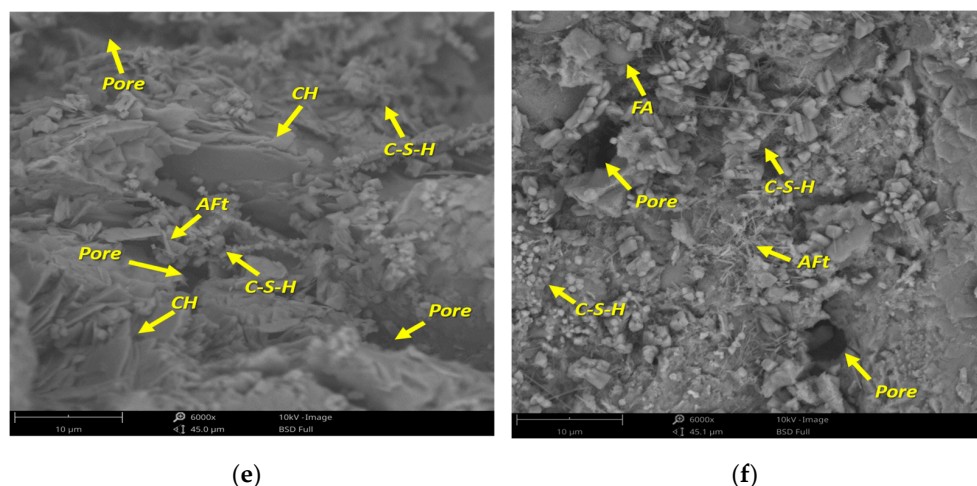


Figure 18. The SEM results of HVFGC's SP addition to the long curing day. (a) 28 days curing day of PCE; (b) 56 days curing day of PCE; (c) 28 days curing day of SNF; (d) 56 days curing day of SNF; (e) 28 days curing day of MLS; (f) 28 days curing day of MLS.

4. Conclusions

- As a result of setting time, the I/F value $W/B = 0.21$, the ratio of PCE to MLS is the same as 4.4~5, and the ratio of $W/B = 0.27$ and 0.35 is the same as the ratio of PCE to SNF, which is 3.3~3.6.
- The optimal ratio was achieved by using PCE, a W/B ratio of 0.21, and FA and GGBFS replacement ratios of 20% and 20%, respectively.
- For the compressive strength of SP types, PCE and SNF can affect the strength development of concrete in 1–7 days, and the strength development after 7 days is more obvious to MLS.
- In the ultrasonic velocity and compressive strength prediction model, the correlation coefficient R value is >0.9 , which is highly reliable, among which the R value of MLS is 0.97 is the best, and its mean squared error is 2.21.

Author Contributions: Conceptualization, W.-T.K. and C.-U.J.; data curation, C.-U.J.; formal analysis, W.-T.K. and C.-U.J.; investigation, W.-T.K.; methodology, W.-T.K. and C.-U.J.; project administration, W.-T.K.; resources, W.-T.K.; supervision, W.-T.K.; validation, W.-T.K. and C.-U.J.; visualization, C.-U.J.; writing—review and editing, W.-T.K. and C.-U.J. All authors have read and agreed to the published version of the manuscript.

Funding: This research was funded by the National Science and Technology Council, grant number: MOST 111-2637-E-992-002.

Institutional Review Board Statement: Not applicable.

Informed Consent Statement: Not applicable.

Data Availability Statement: The study did not report any data availability statement; all data were sourced from real experiments.

Conflicts of Interest: The authors declare no conflict of interest.

References

- Swaroop, A.H.L.; Venkateswararao, K.; Kodandaramarao, P. Durability studies on concrete with fly ash & Ggbs. *Int. J. Eng. Res. Appl.* **2013**, *3*, 285–289.
- Gaur, E.A.S.; Kumar, E.S.; Verma, E.K.P. To Experimental work on concrete properties utilization of marble slurry and ground granulated blast furnace slag by partial replacement of fine aggregate and cement OPC (43-grade). *Int. Res. J. Eng. Technol.* **2017**, *3*, 1196–1201.
- Anant, K.; Krishna, D. Experimental investigation of concrete with cementitious waste material such as GGBS & fly ash over conventional concrete. *Mater. Today Proc.* **2023**, *74*, 953–961. [[CrossRef](#)]

4. Magudeaswaran, P.; Vivek Kumar, C.; Vamsi Krishna, K.; Nagasaibaba, A.; Ravinder, R. Investigational studies on the impact of Supplementary Cementitious Materials (SCM) for identifying the strength and durability characteristics in self curing concrete. *Mater. Today Proc.* **2023**, *21*, 400. [[CrossRef](#)]
5. Zhang, M.H. Microstructure, crack propagation, and mechanical properties of cement pastes containing high volumes of fly ashes. *Cem. Concr. Res.* **1995**, *25*, 165–1178. [[CrossRef](#)]
6. De la Varga, I.; Spragg, R.P.; Di Bella, C.; Castro, J.; Bentz, D.P.; Weiss, J. Fluid transport in high volume fly ash mixtures with and without internal curing. *Cem. Concr. Compos.* **2014**, *45*, 102–110. [[CrossRef](#)]
7. Yao, Z.T.; Ji, X.S.; Sarker, P.K.; Tang, J.H.; Ge, L.Q.; Xia, M.S.; Xi, Y.Q. A comprehensive review on the applications of coal fly ash. *Earth-Sci. Rev.* **2015**, *141*, 105–121. [[CrossRef](#)]
8. Celik, K.; Meral, C.; Mancio, M.; Mehta, P.K.; Monteiro, P.J.M. A comparative study of self-consolidating concretes incorporating high-volume natural pozzolan or high-volume fly ash. *Constr. Build. Mater.* **2014**, *67*, 14–19. [[CrossRef](#)]
9. Malhotra, V.M. High-Performance High-Volume Fly Ash Concrete. *Concr. Int.* **2002**, *24*, 30–34.
10. Mehta, P.K. High-performance, high-volume fly ash concrete for sustainable development. In Proceedings of the International Workshop on Sustainable Development and Concrete Technology, Ames, IA, USA, 14 May 2004; pp. 3–14.
11. Şahmaran, M.; Yaman, İ.Ö.; Tokyay, M. Transport and mechanical properties of self consolidating concrete with high volume fly ash. *Cem. Concr. Compos.* **2009**, *31*, 99–106. [[CrossRef](#)]
12. Dinakar, P.; Babu, K.G.; Santhanam, M. Durability properties of high volume fly ash self compacting concretes. *Cem. Concr. Compos.* **2008**, *30*, 880–886. [[CrossRef](#)]
13. Bouzoubaa, N.; Bilodeau, A.; Tamtsia, B.; Foo, S. Carbonation of fly ash concrete: Laboratory and field data. *Can. J. Civ. Eng.* **2010**, *37*, 1535–1549. [[CrossRef](#)]
14. Mardani-Aghabaglou, A.; Ramyar, K. Mechanical properties of high-volume fly ash roller compacted concrete designed by maximum density method. *Constr. Build. Mater.* **2013**, *38*, 356–364. [[CrossRef](#)]
15. Chen, H.J.; Shih, N.H.; Wu, C.H.; Lin, S.K. Effects of the Loss on Ignition of Fly Ash on the Properties of High-Volume Fly Ash Concrete. *Sustainability* **2019**, *11*, 2704. [[CrossRef](#)]
16. Müllauer, W.; Beddoe, R.E.; Heinz, D. Leaching behaviour of major and trace elements from concrete: Effect of fly ash and GGBS. *Cem. Concr. Compos.* **2015**, *58*, 129–139. [[CrossRef](#)]
17. Wang, L.; Huang, Y.J.; Zhao, F.; Huo, T.T.; Chen, E.; Tang, S.W. Comparison between the influence of finely ground phosphorous slag and fly ash on frost resistance, pore structures and fractal features of hydraulic concrete. *Fractal Fract.* **2022**, *6*, 598. [[CrossRef](#)]
18. Wang, L.; Zhou, S.H.; Shi, Y.; Huang, Y.J.; Zhao, F.; Huo, T.T.; Tang, S.W. The influence of fly ash dosages on the permeability, pore structure and fractal features of face slab concrete. *Fractal Fract.* **2022**, *6*, 476. [[CrossRef](#)]
19. Crossin, E. The greenhouse gas implications of using ground granulated blast furnace slag as a cement substitute. *J. Clean. Prod.* **2015**, *95*, 101–108. [[CrossRef](#)]
20. Suda, V.B.R.; Srinivasa Rao, P. Experimental investigation on optimum usage of Micro silica and GGBS for the strength characteristics of concrete. *Mater. Proc.* **2020**, *27*, 805–811. [[CrossRef](#)]
21. Boubekeur, T.; Boulekbache, B.; Aoudjane, K.; Ezziiane, K.; Kadri, E.H. Prediction of the durability performance of ternary cement containing limestone powder and ground granulated blast furnace slag. *Constr. Build. Mater.* **2019**, *209*, 215–221. [[CrossRef](#)]
22. Jeong, Y.; Park, H.; Jun, Y.; Jeong, J.H.; Oh, J.E. Microstructural verification of the strength performance of ternary blended cement systems with high volumes of fly ash and GGBFS. *Constr. Build. Mater.* **2015**, *95*, 96–107. [[CrossRef](#)]
23. Lim, J.S.; Cheah, C.B.; Ramli, M.B. The setting behavior, mechanical properties and drying shrinkage of ternary blended concrete containing granite quarry dust and processed steel slag aggregate. *Constr. Build. Mater.* **2019**, *215*, 447–461. [[CrossRef](#)]
24. Shubbar, A.A.; Jafer, H.; Dulaimi, A.; Hashim, K.; Atherton, W.; Sadique, M. The development of a low carbon binder produced from the ternary blending of cement, ground granulated blast furnace slag and high calcium fly ash: An experimental and statistical approach. *Constr. Build. Mater.* **2018**, *187*, 1051–1060. [[CrossRef](#)]
25. Cheah, C.B.; Liew, J.J.; Kevin, K.L.P.; Rafat, S.; Weerachart, T. Properties of ternary blended cement containing ground granulated blast furnace slag and ground coal bottom ash. *Constr. Build. Mater.* **2022**, *315*, 125249. [[CrossRef](#)]
26. Shamass, R.; Rispoli, O.; Limbachiya, V.; Kovacs, R. Mechanical and GWP Assessment of Concrete Using Blast Furnace Slag, Silica Fume and Recycled Aggregate. *Case Stud. Constr. Mater.* **2023**, *24*, e02164. [[CrossRef](#)]
27. Weise, K.; Ukrainczyk, N.; Duncan, A. Eduardus Koenders, Enhanced Metakaolin Reactivity in Blended Cement with Additional Calcium Hydroxide. *Materials* **2022**, *15*, 367. [[CrossRef](#)]
28. Izadifar, M.; Thissen, P.; Steudel, A.; Kleeberg, R.; Kaufhold, S.; Kaltenbach, J.; Schuhmann, R.; Dehn, F.; Emmerich, K. Comprehensive examination of dehydroxylation of kaolinite, disordered kaolinite, and dickite: Experimental studies and density functional theory. *Clays Clay Miner.* **2020**, *68*, 319–333. [[CrossRef](#)]
29. ASTM C150; Standard Specification for Portland Cement. ASTM International: West Conshohocken, PA, USA, 2022.
30. ASTM C618; Standard Specification for Coal Fly Ash and Raw or Calcined Natural Pozzolan for Use in Concrete. ASTM International: West Conshohocken, PA, USA, 2022.
31. ASTM C989; Standard Specification for Ground Granulated Blast-Furnace Slag for Use in Concrete and Mortars. ASTM International: West Conshohocken, PA, USA, 2010.
32. ASTM C33; Standard Specification for Concrete Aggregates. ASTM International: West Conshohocken, PA, USA, 2012.

33. ASTM C305; Standard Practice for Mechanical Mixing of Hydraulic Cement Pastes and Mortars of Plastic Consistency. ASTM International: West Conshohocken, PA, USA, 2020.
34. ASTM C807; Standard Test Method for Time of Setting of Hydraulic Cement Mortar by Modified Vicat Needle. ASTM International: West Conshohocken, PA, USA, 2021.
35. ASTM C109; Standard Test Method for Compressive Strength of Hydraulic Cement Mortars (Using 2-in. or [50 mm] Cube Specimens). ASTM International: West Conshohocken, PA, USA, 2021.
36. ASTM C348; Standard Test Method for Flexural Strength of Hydraulic-Cement Mortars. ASTM International: West Conshohocken, PA, USA, 2021.
37. ASTM C597; Standard Test Method for Pulse Velocity Through Concrete. ASTM International: West Conshohocken, PA, USA, 2016.
38. ASTM C1585; Standard Test Method for Measurement of Rate of Absorption of Water by Hydraulic-Cement Concretes. ASTM International: West Conshohocken, PA, USA, 2020.
39. Ke, G.J.; Zhang, X.; Zhang, J. Hydration characteristics of calcium sulfoaluminate-fly ash mixed with different alkalies. *Case Stud. Constr. Mater.* **2022**, *17*, e01478. [[CrossRef](#)]
40. Juang, C.U.; Kuo, W.T. Engineering Properties of Green and Ecofriendly Grouting Materials with Different Sand Filling Ratios. *Materials* **2023**, *16*, 837. [[CrossRef](#)]
41. Manojsuburam, R.; Sakthivel, E.; Jayanthimani, E. A study on the mechanical properties of alkali activated ground granulated blast furnace slag and fly ash concrete. *Mater. Proc.* **2022**, *62*, 1761–1764. [[CrossRef](#)]
42. Shi, Y.X.; Xue, C.H.; Jia, Y.L.; Guo, W.C.; Zhang, Y.Y.; Qiu, Y.X.; Zhao, Q.X. Preparation and curing method of red mud-calcium carbide slag synergistically activated fly ash-ground granulated blast furnace slag based eco-friendly geopolymer. *Cem. Concr. Compos.* **2023**, *23*, 104999. [[CrossRef](#)]
43. Jiao, Z.Z.; Li, X.Y.; Yu, Q.L.; Yao, Q.Q.; Hu, P. Sulfate resistance of class C/class F fly ash geopolymers. *J. Mater. Res. Technol.* **2023**, *23*, 1767–1780. [[CrossRef](#)]
44. Joanna, P.S.; Parvati, T.S.; Rooby, J.; Preetha, R. A study on the flexural behavior of sustainable concrete beams with high volume fly ash. *Mater. Proc.* **2020**, *33*, 1149–1157. [[CrossRef](#)]
45. Dragaš, J.; Marinković, S.; Ignjatović, I.; Tošić, N.; Koković, V. Flexural behaviour and ultimate bending capacity of high-volume fly ash reinforced concrete beams. *Eng. Struct.* **2023**, *277*, 115446. [[CrossRef](#)]
46. Yoo, S.W.; Ryu, G.S.; Choo, J.F. Evaluation of the effects of high-volume fly ash on the flexural behavior of reinforced concrete beams. *Constr. Build. Mater.* **2015**, *93*, 1132–1144. [[CrossRef](#)]
47. Narendra, B.K.; Mahadeviah, T.M. Flexural behavior of reinforced fly ash concrete in comparison to reinforced normal concrete beams in terms of cracking load and ultimate load carrying capacity. *Int. J. Eng. Adv. Technol.* **2014**, *4*, 7–40.
48. Hashmi, A.F.; Shariq, M.; Baqi, A. Flexural performance of high volume fly ash reinforced concrete beams and slabs. *Structures* **2020**, *25*, 868–880. [[CrossRef](#)]

Disclaimer/Publisher's Note: The statements, opinions and data contained in all publications are solely those of the individual author(s) and contributor(s) and not of MDPI and/or the editor(s). MDPI and/or the editor(s) disclaim responsibility for any injury to people or property resulting from any ideas, methods, instructions or products referred to in the content.